

Preparation and Properties of Cyclo-Olefin Copolymer/Titania Hybrids

Cheng-Fang Ou, Ming-Chieh Hsu

Department of Chemical and Materials Engineering, National Chin-Yi University of Technology, Taichung County 411, Taiwan, Republic of China

Received 15 June 2007; accepted 29 December 2007

DOI 10.1002/app.28529

Published online 10 July 2008 in Wiley InterScience (www.interscience.wiley.com).

ABSTRACT: A series of organic–inorganic hybrid materials consisting of an organic cyclo-olefin copolymer (COC) and inorganic titania (TiO_2) were successfully synthesized by a sol–gel process. TiO_2 was obtained through the hydrolysis of titanium *n*-butoxide (TNBT) with the catalysis of HCl. Differential scanning calorimetry analysis indicated that the glass-transition temperature of the hybrids was higher than that of pure COC, and it rose significantly as the TNBT content was increased from 1 to 15 wt %. Scanning electron microscopy observations showed that the morphology of fractured surfaces of the COC/ TiO_2 hybrid with 5 wt % TNBT was a single homogeneous phase, indicating that the miscibility between COC and TiO_2 was good

for the hybrids. According to ultraviolet–visible analysis, the transmittance of pure COC at 550 nm was high up to 91.7%. The light transmittance of the COC/ TiO_2 hybrids was still higher than 80% with the TNBT content up to 5 wt %. The decomposition temperatures of the hybrids, investigated with thermogravimetric analysis, were not affected significantly by the addition of TNBT. The oxygen barrier property of the hybrid films showed significant improvements in comparison with pure COC. © 2008 Wiley Periodicals, Inc. *J Appl Polym Sci* 110: 732–737, 2008

Key words: FTIR; morphology; thermogravimetric analysis (TGA)

INTRODUCTION

The copolymerization of norbornene with ethylene, leading to cyclo-olefin copolymers (COCs) with unique physical properties, has been reported.^{1–6} These products, which are highly optically transparent and have high glass-transition temperatures (T_g 's), high decomposition temperature (T_d 's), and good moisture barrier and mechanical properties, are potential replacements for polycarbonate as engineering plastics. These novel polymers have potential applications in optical fiber and transparent engineering thermoplastics, just like polycarbonate. Increasing the ethylene content in COCs results in a higher melt-flow rate, and they can be processed like most thermoplastics in extrusion and injection molding.^{7–10} The manufacture and properties of COCs have been studied extensively with experimental techniques, with a focus on the improvement of manufacturing technologies.^{11–13}

Polymer substrates have been widely used in the flat-panel-display industry because of their flexibil-

ity, light weight, and high power efficiencies. However, there are some technological difficulties in achieving a display on a polymer substrate, such as lower thermal stability and higher water/oxygen permeation.^{14–18}

Lately, many researchers have devoted great effort to the sol–gel technique to prepare ceramic precursors and inorganic glasses at relatively low temperatures. This technique has attracted intense research interest because of its potential for developing new ceramics or glasses. At present, the sol–gel method is not only a manufacturing process for homogeneous inorganic glasses but also a technique for the synthesis of organic–inorganic hybrid materials for various applications, including optical and nonlinear devices, electrical, organically modified ceramic materials, reinforced elastomers and plastics, and biochemical purposes.^{19–24} In these applications, important properties, such as the appearance, transparency, and phase behavior, depend on the development of an inorganic silicate structure and the interfacial interactions between the organic and inorganic phases in the hybrid materials. The silica (SiO_2) molecules act as reinforcing agents, making the polymers harder, giving them better mechanical properties, improving their thermal stability, and lowering the water/oxygen permeation and coefficient of thermal expansion. Hence, studies on these topics are very important for the advancement of

Correspondence to: C.-F. Ou (oucf@ncut.edu.tw).

Contract grant sponsor: National Science Council of Republic of China; contract grant number: NSC94-2216-E-167-002.

this technology. Many studies have been devoted to the preparation of polymer/SiO₂ hybrid materials with organic monomers and inorganic precursors such as tetraethyloxysilane through *in situ*, acid-catalyzed sol-gel processes.^{25–28} The preparation and properties of COC/SiO₂ hybrid materials have been reported in our previous research.²⁹ In these hybrids, the inorganic molecules and organic molecules are interconnected by chemical covalent bonds, hydrogen bonds, or physical interactions. The structure of a hybrid depends on the processing conditions, such as the type of catalyst, the pH value, the water quantity, the solvent system, and the reaction temperature. The as-prepared composites can be changed from soft and flexible materials to brittle and hard materials according to the chemical structures of the organic components and the overall composition ratio of the organic and inorganic moieties.

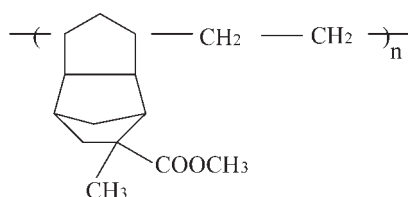
Recently, organic-inorganic hybrid materials containing titania (TiO₂) have gradually attracted obvious research attention because of their characteristically high refractive index. Some studies of polymer/TiO₂ hybrid systems have been reported. For example, Mark et al.³⁰ reported the preparation and properties of poly(phenylene terephthalate)-TiO₂ hybrid materials. Wang and Wilkes³¹ reported the preparation and properties of poly(tetramethylene oxide)-TiO₂ hybrid materials. Lee and Chen³² reported the preparation of high-refractive-index poly(methyl methacrylate)-TiO₂ hybrid materials with 3-(trimethoxysilyl)propyl methacrylate as coupling agent.

In this study, COC/TiO₂ hybrids were constructed from COC and inorganic titanium *n*-butoxide [TNBT or Ti(OC₄H₉)₄] prepared via an acid-catalyzed sol-gel process. The effects of the material composition on the thermal properties, thermal stability, light transmittance, morphology, and oxygen permeability were studied with differential scanning calorimetry (DSC), thermogravimetric analysis (TGA), ultraviolet-visible (UV-vis) transmission spectroscopy, scanning electron microscopy (SEM), and gas permeability analysis, respectively.

EXPERIMENTAL

Materials

The COC copolymer was a commercial product (Arton F4520) manufactured by Japan Synthetic Rubber Co., Ltd. (JSR, Japan). The chemical structure of COC can be shown as follows:



TNBT [Across], tetrahydrofuran (Fisher), acetyl acetone (ACAC; Fluka, Switzerland), and hydrochloric acid (HCl; Showa Chemical, Japan) were used as received without further purification. Deionized water was generated with the Milli-Q Plus water purification system (Millipore).

Preparation of the desired hybrid films

COC was dissolved in tetrahydrofuran first. A homogeneous solution of TNBT and ACAC (functioning as a chelating agent) was then prepared with an ACAC/H₂O/TNBT/H⁺ molar ratio of 1/4/1/0.05. Various organic-inorganic ratios (99/1, 95/5, 90/10, and 85/15 w/w) for the COC/TNBT mixture were stirred for 1 h at room temperature, poured into a sealed reactor, and allowed to react at 55°C for 6 h. After the sol-gel reaction, the mixture was removed from the reactor and poured into an aluminum mold, and then it was dried at 70°C *in vacuo* for 24 h. The postreaction was conducted at 105°C *in vacuo* for 24 h to remove any residual solvent and byproducts (water and alcohol). For comparison, pure COC was also made with the same procedure.

Characterization

DSC measurements were performed with a TA 2010 analyzer (TA Instruments, New Castle, DE). Each sample was dried at 60°C for 6 h in a vacuum oven before DSC characterization. Appropriate amounts of samples (ca. 5 mg) were sealed in aluminum sample pans. DSC analyses of these hybrid materials were then conducted under a dry nitrogen atmosphere. The samples were heated first to 250°C and kept there for 3 min in a hermetic cell to remove the thermal history. The samples were then cooled to 30°C at the rate of 20°C/min, and then a second heating was performed at the rate of 20°C/min to 250°C. The *T_g* results from the second heating thermograms were the averages of three samples. TGA of the dried hybrids was performed with a TA Q500 (TA Instruments, New Castle, DE) under a nitrogen atmosphere at a heating rate of 20°C/min.

The morphology of the hybrid material was obtained from SEM observations with a JEOL JSM-6360. The structural characteristics of the raw materials and hybrids were analyzed with a Nicolet Avatar 320 Fourier transform infrared (FTIR) spectrometer in the special range of 4000–400 cm⁻¹ with a 4-cm⁻¹ resolution. The optical transmittance analysis was measured with a Varian Cary-100 UV-vis spectrometer with wavelengths ranging from 300 to 800 nm.

The oxygen permeability of hybrid films was determined with a Yanaco GTR-10 gas permeability analyzer (YANACO Group, Japan). The thicknesses of these films were about 100 μm. The test was

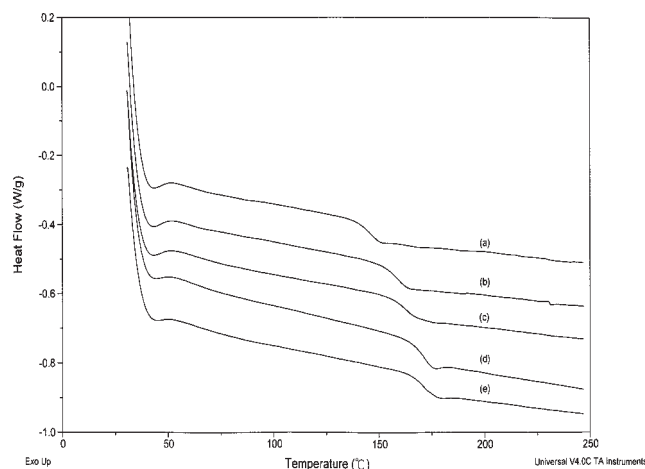


Figure 1 DSC thermogram curves of the pure COC and COC/TiO₂ hybrids: (a) pure COC and (b) 1, (c) 5, (d) 10, and (e) 15 wt % TNBT.

carried out under isothermal conditions at 35°C, and the pressure was 50 kPa. Permeability is usually expressed in barrers [10^{-10} cm³ (STP) cm/cm² s cmHg].

RESULTS AND DISCUSSION

T_g of the hybrids

DSC was introduced to investigate T_g of these hybrids. Figure 1 shows the DSC thermogram curves of neat COC and hybrid materials. A distinct single T_g is located in the region from 146 to 171.9°C for all the hybrids, and the T_g values are listed in Table I. T_g of pure COC was 146°C. The T_g values of the hybrids were higher than that of pure COC. The T_g values of these hybrids rose with an increasing amount of inorganic TiO₂ in the hybrids. The extremely high value of T_g was 171.9°C, 25.9°C higher than that of pure COC, when the TNBT content was increased to 15 wt %. The increasing cross-linking density of the hybrids with the TNBT concentration increasing from 1 to 15 wt %, due to the developed inorganic TiO₂ structure, brought about a reduction of molecular mobility and an elevation of T_g .^{33–35} In the COC/tetraethyloxysilane hybrids,²⁶ all the synthesized hybrids had IR absorption at about 1728 cm⁻¹, which corresponded to the carbonyl group C=O stretching vibration on the side chain of COC. This absorption was constructed by two distinct peaks at about 1728 and 1710 cm⁻¹, which belonged to free and hydrogen-bonded carbonyl groups, respectively. In the COC/TiO₂ hybrids, the T_g 's of hybrids increased significantly with the TiO₂ loading increasing. The most likely reason is that the specific interaction of hydrogen bonding between the TiO₂ network and polymer

TABLE I
 T_g , T_d , and Char Yield of the Pure COC and COC/TiO₂ Hybrids

Composition	T_g (°C)	T_d (°C) ^a	TiO ₂ (wt %)	wt _R ⁷⁰⁰ ^b
Pure COC	146.0	474.7	0.0	0.3
1 wt % TNBT	157.4	476.5	0.2	0.5
5 wt % TNBT	162.9	472.3	1.3	1.6
10 wt % TNBT	169.9	471.9	2.4	2.7
15 wt % TNBT	171.9	476.5	3.7	3.9
TiO ₂	—	—	—	51.4

^a Degradation temperatures were obtained from the peaks of the DTG data.

^b Weight percentage residue at 700°C.

matrix effectively restricted the mobility of the COC chains.

Thermal stability of the hybrids

Figure 2 illustrates the TGA curves of the hybrids at a heating rate of 20°C/min under a nitrogen flow. The data for the degradation temperatures were collected from derivative thermogravimetry (DTG) curves (not shown) and are listed in Table I. We found that COC decomposed in a single stage (main degradation stage) and that its T_d was 474.7°C. In the COC/TiO₂ hybrids, there were two stages of weight loss. The first stage of degradation (predegradation stage), occurring at 180–230°C, was probably due to the evaporation of the residual solvent and physically absorbed water. The main degradation stage started at about 450°C, and it was attributed to the decomposition of the polymer.

It was observed that T_d of the hybrids was about the same as that of pure COC. The weight of the residue in the hybrids at 700°C was proportional to the

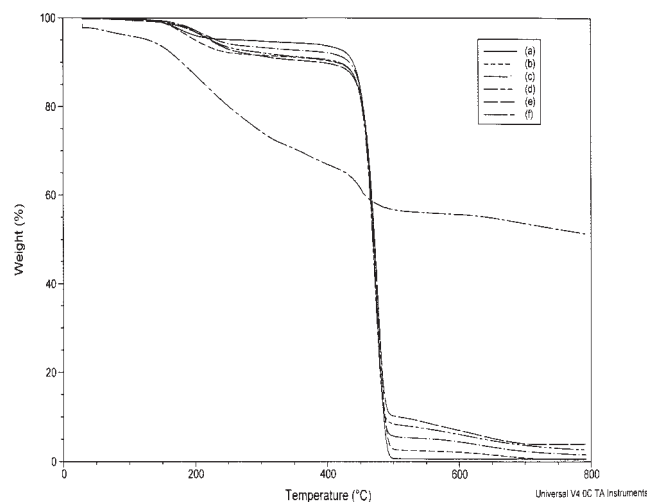


Figure 2 TGA curves of the pure COC and COC/TiO₂ hybrids: (a) pure COC; (b) 1, (c) 5, (d) 10, and (e) 15 wt % TNBT; and (f) TiO₂.

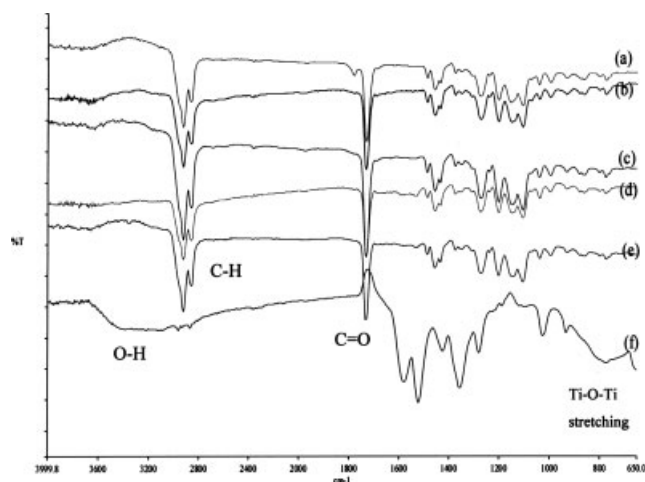


Figure 3 FTIR spectra of the pure COC and COC/TiO₂ hybrids: (a) pure COC; (b) 1, (c) 5, (d) 10, and (e) 15 wt % TNBT; and (f) TiO₂.

titanium content, and the residual components were mostly titanium dioxide. Table I also shows that the quantity of the residue in the hybrids at 700°C

increased with increasing TNBT content. On this basis, the amounts of TiO₂ formed in the hybrids could be determined. The calculated results are listed in Table I. The amount of TiO₂ in the hybrids increased with increasing TNBT content.

FTIR characterization

The IR spectra of the raw material and hybrids are shown in Figure 3. As shown in Figure 3, the absorption peaks of the stretching vibration bands of the C=O and C—H bonds in the COC segment are at about 1728 and 2950 cm⁻¹, respectively. The Ti—OH band in the spectra of TNBT can be observed as a broad absorption in the range of 3000–3600 cm⁻¹. The broad absorption bands in TNBT at about 650–850 cm⁻¹ correspond to Ti—O—Ti stretching vibrations in IR spectra.³⁶ There is no Ti—O—Ti band in the network of hybrid materials because of the steric hindrance of COC and the low content of TNBT in the hybrids.

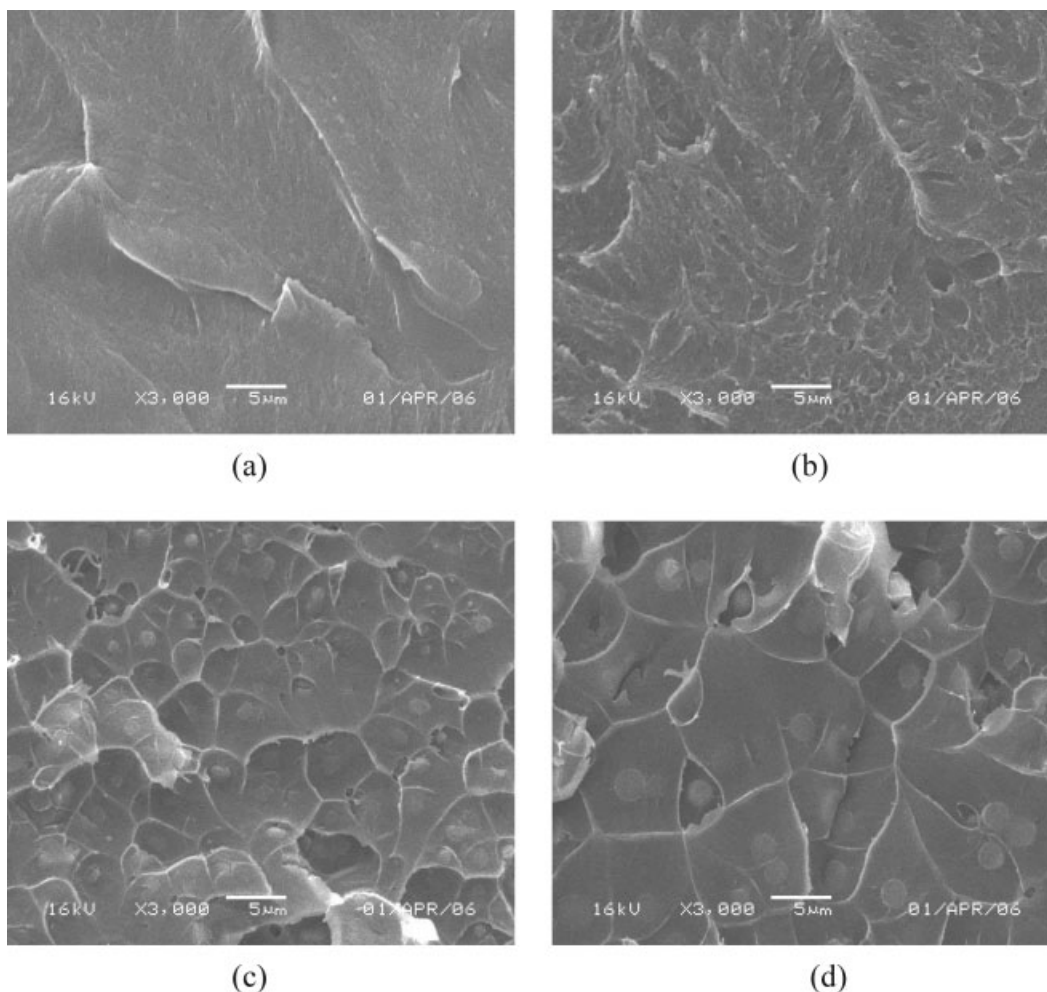


Figure 4 SEM micrographs of the fracture surfaces of the COC/TiO₂ hybrids: (a) 1, (b) 5, (c) 10, and (d) 15 wt % TNBT.

Morphology investigation

A transparent and smooth specimen was obtained for pure COC and a hybrid with less than 5 wt % TNBT. A 10 wt % TNBT specimen was translucent, and a 15 wt % TNBT specimen was opaque. It was concluded that the organic and inorganic phases were compatible in the COC/TiO₂ hybrids with TNBT concentrations lower than 5 wt %.

Figure 4 shows SEM micrographs of the fracture surfaces of the samples. The fractured surfaces of hybrids with 1 and 5 wt % TNBT were smooth and homogeneous [Fig. 4(a,b)]. This result indicates that miscibility between COC and TiO₂ was good for the hybrids with TNBT concentrations lower than 5 wt %. In Figure 4(c,d), the morphology of the COC/TiO₂ hybrids with 10 and 15 wt % TNBT shows an obvious change from that of the 1 wt % TNBT hybrid. The dispersed droplet dispersions of TiO₂ were embedded in the COC matrix. The shapes of the dispersed droplets were spherical or elliptical geometries, with the domain sizes ranging from 1 to 3 μm . The size of the dispersed droplets in the 15 wt % TNBT hybrid was larger than that in the 10 wt % TNBT hybrid.

Transmittance of the hybrids

Figure 5 shows the UV-vis spectra for pure COC and COC/TiO₂ hybrids. The thickness of these films was about 100 μm . The transmittance of pure COC at 550 nm was as high as 91.7%. The spectra show that the visible region (400–700 nm) was not affected by the presence of less than 5 wt % TNBT and retained the high transparency of COC. The transmittance of the 5 wt % TNBT hybrid was still higher than 80% at 550 nm. The transmittance of the 10 wt

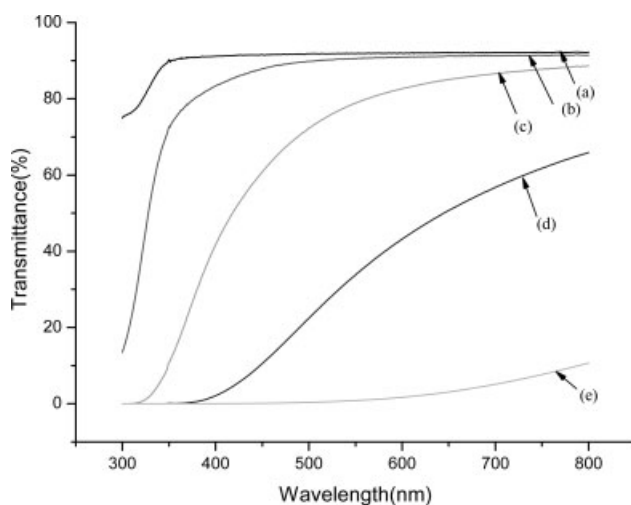


Figure 5 Transmittance spectra of the pure COC and COC/TiO₂ hybrids: (a) pure COC and (b) 1, (c) 5, (d) 10, and (e) 15 wt % TNBT.

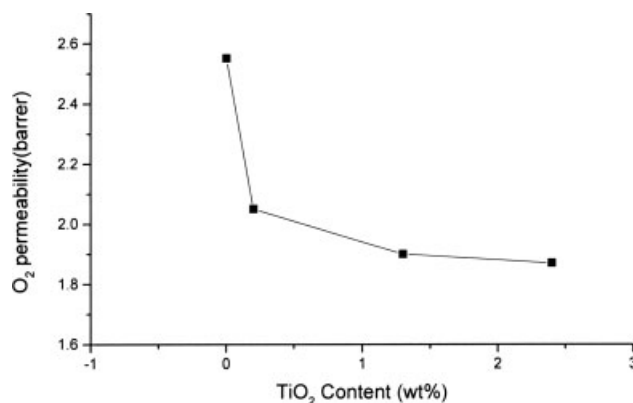


Figure 6 Oxygen permeability of the pure COC and COC/TiO₂ hybrids.

% TNBT hybrid decreased abruptly to 32% at 550 nm and was opaque for 15 wt % TNBT. As shown in the SEM micrograph of the 15 wt % TNBT hybrid [Fig. 4(d)], the large size (1–3 μm) and higher content of TiO₂ droplets dispersed in the COC matrix resulted in lower light transmittance. The finer size of TiO₂, accompanied by good compatibility between TiO₂ and COC, might be the reason for the high light transmittance of the COC/TiO₂ hybrid with less than 5 wt % TNBT.

Oxygen permeability study

Figure 6 presents the TNBT content dependence of the oxygen permeability of COC/TiO₂ hybrids with respect to pure oxygen at 35°C. The oxygen permeability decreased with an increasing amount of TNBT. The oxygen permeability of the pure COC and COC/TiO₂ hybrids were 2.55, 2.05, 1.90, and 1.87 barrers for pure COC and 1, 5, and 10 wt % TNBT hybrids. The reduction of oxygen permeability decreased with the concentration of TNBT increasing to 10 wt %. In the 10 wt % TNBT hybrid, there was a significant decrease of 27% in the oxygen permeability, indicating a significantly improved oxygen barrier property of COC. The reduction of permeability arose from the longer diffusive path that the penetrants had to travel in the presence of the nanoparticles.

CONCLUSIONS

In this study, COC/TiO₂ hybrids exhibited higher T_g values than pure COC, and T_g rose as the TNBT content increased. The extremely high value of T_g was 171.9°C, 25.9°C higher than that of pure COC, when the TNBT content was increased to 15 wt %. The COC/TiO₂ hybrids exhibited the same thermal resistance as the pure COC polymer. The light transmittance of the COC/TiO₂ hybrids was still higher

than 80% as the TNBT content increased to 5 wt %. The oxygen barrier property of the hybrid films showed significant improvements in comparison with pure COC.

References

1. Katajisto, J.; Linnolahti, M.; Pakkanen, T. A. *Theor Chem Acc* 2005, 113, 281.
2. Marathe, S.; Mohandas, Y. P.; Sivaram, S. *Macromolecules* 1995, 28, 7318.
3. Harrington, B. A.; Crowther, D. J. *J Mol Cat A* 1998, 128, 79.
4. Kaminsky, W. *Papra Rev Rep* 1999, 10, 28.
5. Yeh, J. M.; Weng, C. J.; Huang, K. Y.; Huang, H. Y.; Yu, Y. H. *J Appl Polym Sci* 2004, 94, 400.
6. Huang, W. J.; Chang, F. C. *J Polym Res* 2003, 10, 195.
7. Kaminsky, W.; Bark, A.; Arndt, M. *Macromol Chem Macromol Symp* 1991, 47, 83.
8. Kaminsky, W.; Bark, A. *Polym Int* 1992, 28, 251.
9. Herfert, N.; Montag, P.; Fink, G. *Macromol Chem* 1993, 194, 3167.
10. Kaminsky, W. *Macromol Chem Phys* 1996, 197, 3907.
11. Alt, F. P.; Heitz, W. *Acta Polym* 1998, 49, 477.
12. Ruchatz, D.; Fink, G. *Macromolecules* 1998, 31, 4681.
13. Kaminsky, W. *Catal Today* 1994, 20, 257.
14. Burrows, P. E.; Graff, G. L.; Gross, M. E.; Martin, P. M.; Shi, M. K.; Hall, M.; Mast, E.; Bonham, C.; Bennett, W.; Sullivan, M. B. *Display* 2001, 22, 65.
15. Kloppel, M.; Kriegeis, W.; Meyer, B. K.; Scharmann, A.; Daube, C.; Stollenberg, J.; Tube, J. *Thin Solid Films* 2000, 365, 139.
16. Fahland, M.; Karlsson, P.; Charton, C. *Thin Solid Films* 2001, 392, 334.
17. Lee, M. J.; Judge, C. P.; Wright, S. W. *Solid-State Electron* 2000, 44, 1431.
18. Henry, B. M.; Erlat, A. G.; McGuigan, A.; Grovenor, C. R. M.; Briggs, G. A. D.; Tsukahara, Y.; Miyamoto, T.; Nijima, T. *Thin Solid Films* 2001, 382, 194.
19. Brinker, C. J.; Scherer, G. W. *Sol-Gel Science: The Physics and Chemistry of Sol-Gel Processing*; Academic: London, 1990.
20. Hoh, K. P.; Ishida, H.; Koenig, J. L. *Polym Compos* 1990, 11, 121.
21. Bahulekar, R. V.; Prabhune, A. A.; Sivaraman, H.; Ponrathnam, S. *Polymer* 1993, 34, 163.
22. Novak, B. M. *Adv Mater* 1993, 5, 422.
23. Zarzycki, J. *J Sol-Gel Sci Technol* 1997, 8, 17.
24. Calvert, P. *Nature* 1991, 353, 501.
25. Weetall, H. H.; Robertson, B.; Cullin, D.; Brown, J.; Walch, M. *Biochim Biophys Acta* 1993, 1142, 211.
26. Reetz, M. T.; Zonta, A.; Simpelkamp, J. *Biotechnol Bioeng* 1996, 49, 527.
27. Park, S. H.; Lee, S. B.; Ryu, D. D. Y. *Biotechnol Bioeng* 1981, 23, 2591.
28. Ruckenstein, E.; Wang, X. *Biotechnol Bioeng* 1992, 39, 679.
29. Ou, C. F.; Hsu, M. C. *J Appl Polym Sci* 2007, 104, 2542.
30. Ahmad, Z.; Sarwar, M. I.; Wang, S.; Mark, J. E. *Polymer* 1997, 38, 4523.
31. Wang, B.; Wilkes, G. L. *J Polym Sci Part A: Polym Chem* 1991, 29, 905.
32. Lee, L. H.; Chen, W. C. *Chem Mater* 2001, 13, 1137.
33. Norisuye, T.; Shibayama, M.; Tamaki, R.; Chujo, Y. *Macromolecules* 1999, 32, 1528.
34. Chan, C. K.; Chu, I. M.; Lee, W.; Chin, W. K. *Macromol Chem Phys* 2001, 202, 911.
35. Chan, C. K.; Chu, I. M.; Ou, C. F.; Lin, Y. W. *Mater Lett* 2004, 58, 2243.
36. Lee, L. H.; Chen, W. C. *Chem Mater* 2001, 13, 1137.